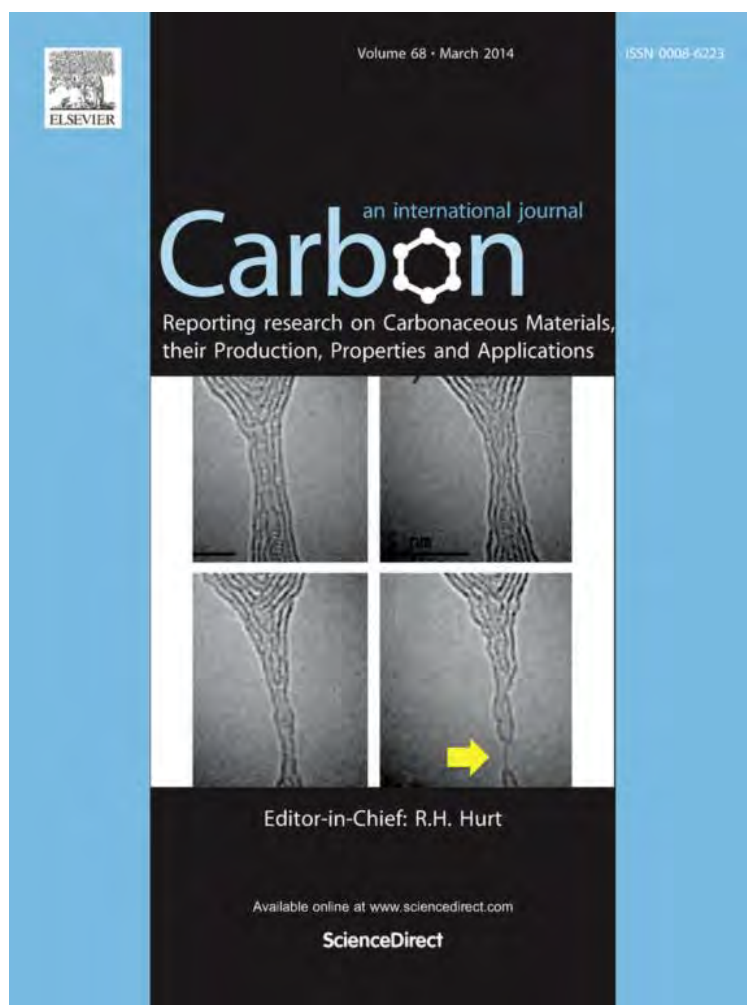


Provided for non-commercial research and education use.
Not for reproduction, distribution or commercial use.



This article appeared in a journal published by Elsevier. The attached copy is furnished to the author for internal non-commercial research and educational use, including for instruction at the author's institution and sharing with colleagues.

Other uses, including reproduction and distribution, or selling or licensing copies, or posting to personal, institutional or third party websites are prohibited.

In most cases authors are permitted to post their version of the article (e.g. in Word or Tex form) to their personal website or institutional repository. Authors requiring further information regarding Elsevier's archiving and manuscript policies are encouraged to visit:

<http://www.elsevier.com/copyright>

Available at www.sciencedirect.com

ScienceDirect

journal homepage: www.elsevier.com/locate/carbon

Interface-derived extraordinary viscous behavior of exfoliated graphite



D.D.L. Chung *

Composite Materials Research Laboratory, University at Buffalo, State University of New York, Buffalo, NY 14260-4400, United states

ARTICLE INFO

Article history:

Received 4 October 2013

Accepted 16 November 2013

Available online 25 November 2013

ABSTRACT

Exfoliated graphite is obtained by the rapid heating of acid-intercalated graphite flakes. It exhibits a cellular microstructure, with about 60 graphite layers in the cell wall. The recently reported extraordinarily strong viscous behavior of the exfoliated graphite and its cement-matrix composite has been explained in this paper in terms of an interface-derived viscous mechanism, which is in contrast to the well-known bulk viscous deformation mechanism that rubber exhibits. The interfacial mechanism is associated with the dynamic sliding at low amplitudes between the graphite layers in the cell wall of exfoliated graphite during dynamic loading in the elastic regime. The ease of sliding is enabled by the loosening of the interlayer interface that has occurred during exfoliation, in which the cell wall extends greatly like a balloon due to extensive sliding between the graphite layers in the cell wall. The viscous behavior is consistent with the well-known resiliency of flexible graphite, which is a sheet made by greatly compressing exfoliated graphite without a binder. In the cement-matrix composite, the exfoliated graphite is sandwiched with sufficient tightness by the cement matrix in the microstructure of the composite, thereby providing constrained-layer damping in the microscale.

© 2013 Elsevier Ltd. All rights reserved.

1. Introduction

Viscous behavior that is extraordinarily strong among solids has been recently reported in exfoliated graphite in the small-strain elastic regime [1]. Furthermore, the incorporation of the exfoliated graphite in a cement-matrix composite has been reported to provide a material that exhibits an exceptionally high level of vibration damping [2], provided that the units of exfoliated graphite are sandwiched sufficiently tightly by the cement matrix [3]. Although the behavior has been reported, the scientific origin of the behavior has not been enunciated. This paper is directed at elucidating the scientific origin of the above mentioned phenomena, which have opened up applications for exfoliated graphite in vibra-

tion damping, vibration isolation and possibly sound absorption as well.

2. Exfoliated graphite

Exfoliated graphite exhibits a cellular microstructure [4–7] (Fig. 1), which results from the exfoliation of intercalated graphite [4,8,9]. Intercalated graphite is graphite which has been reacted with a foreign species, called the intercalate. The reaction is known as intercalation. The reaction causes the intercalate to enter the space, typically as a monolayer, between the atomic layers in the graphite, thereby forming a layered compound known as an intercalation compound. Due to their crystallinity and low cost, natural graphite flakes

* Fax: +1 716 645 2883.

E-mail address: ddlchung@buffalo.eduURL: <http://alum.mit.edu/www/ddlchung>.

0008-6223/\$ - see front matter © 2013 Elsevier Ltd. All rights reserved.

<http://dx.doi.org/10.1016/j.carbon.2013.11.045>

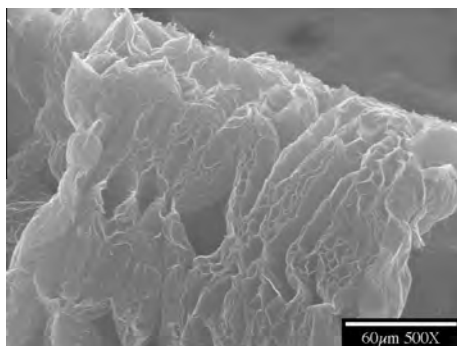


Fig. 1 – SEM microscope photograph of exfoliated graphite used in the discovery of interface-derived extraordinary viscous behavior of exfoliated graphite [1,2]. It shows the well-known cellular microstructure. A worm is a piece of exfoliated graphite obtained by the exfoliation of a single graphite flake. Only a part of a worm is shown. The exfoliation was conducted by rapid heating of acid-intercalated graphite flakes.

are most commonly used to prepare exfoliated graphite. There is typically a charge transfer that occurs between the intercalate and the graphite. Most commonly, the intercalate accepts electrons from the graphite, as in the case of sulfuric acid as the intercalate [10]. In fact, sulfuric and nitric acids are the most commonly used intercalates for preparing exfoliated graphite, due to the large degree of irreversible expansion that stems from the gaseous species generated by the decomposition of the acid molecules during exfoliation [11].

The intercalate is typically present in the form of islands, in accordance with the Daumas-Herold model [12], in which the graphite layers bend, thereby resulting in domains, each of which is an intercalate island (Fig. 2). This model has been confirmed by electron microscopy [13,14]. It means that, for stages greater than 1, the intercalate layer does not necessarily extend all the way from one end of the graphite crystal to the other. The in-plane length of an island depends on the intercalate species and the intercalate activity during intercalation. For the same intercalate species, the lower is the intercalate activity (as obtained by increasing the intercalation temperature or decreasing the intercalate concentration in the reaction vessel during intercalation), the larger are the intercalate islands [15].

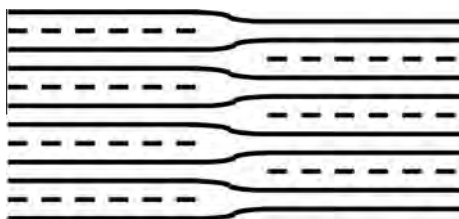


Fig. 2 – Daumas-Herold Model [12] as illustrated for a stage-2 graphite intercalation compound. The stage refers to the number of graphite layers between nearest intercalate layers in the superlattice along the c-axis. The graphite layers are indicated by solid lines; the intercalate layers are indicated by dotted lines.

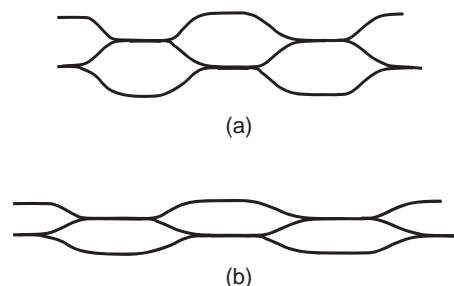


Fig. 3 – Schematic illustration (not to scale) of the cellular structure of exfoliated graphite. The cell wall, which is a nanoscale multilayer that consists of about 60 graphite layers, can stretch greatly due to the sliding of the graphite layers with respect to one another. The solid line denotes the cell wall. The individual layers in the multilayer are not shown. (a) Before loading. (b) During loading.

During the heating of intercalated graphite, each intercalate island expands tremendously along the c-axis of the graphite. The larger are the intercalate islands, the greater is the degree of expansion [15]. Thus, for a high degree of exfoliation, the lateral size of the graphite flakes must be large enough to accommodate at least several islands in the plane of the flake. The expansion can be up to a few hundred times, depending on the choice of intercalate and the size of the intercalate islands [10,15–17]. The driving force of the expansion is the vaporization or decomposition of the intercalate upon heating [10,15]. Thermal decomposition that causes an intercalate molecule to decompose into multiple molecules helps enhance the gas evolution during exfoliation, thereby increasing the driving force. An exfoliated graphite flake is known as a worm, due to its shape.

In order for the large expansion to be able to occur during exfoliation, the graphite layers that make up the wall of an intercalate island must be able to stretch greatly – akin to the stretching of the wall of a balloon as it expands (Fig. 3). The stretching of the wall enables an intercalate island to expand like a balloon. A wall consists of multiple layers of graphite, such that each layer does not necessarily extend all the way across the length of an island and different layers may overlap one another to various degrees (Fig. 4). The structure of the wall has not been adequately addressed. There are about 60 graphite layers (on the average) in the cell wall of the exfoliated graphite used in the discovery of the extraordinary viscous behavior of exfoliated graphite [1]. The stretching of a wall is made possible by the sliding of the graphite layers with respect to one another within the wall. This sliding requires the overcoming of the van der Waals' forces between the graphite layers. The vapor-related driving force for exfoliation is adequate for overcoming these forces, thereby allowing exfoliation to occur. If the heating rate during exfoliation is high enough and the vapor evolution during exfoliation is significant enough, the expansion is substantially irreversible, so that the expanded state remains upon subsequent cooling. This is the case when acids are used as the intercalates [10,11,15], since an acid molecule decomposes upon heating. The term “exfoliated graphite” typically refers to the irreversibly expanded form.

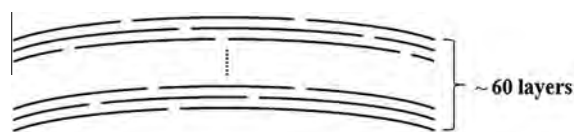


Fig. 4 – Schematic illustration of the structure in a cell wall of exfoliated graphite. There are about 60 graphite layers in a cell wall of the exfoliated graphite used in the discovery of interface-derived extraordinary viscous behavior of exfoliated graphite [1,2].

3. Interface-derived extraordinary viscous behavior of exfoliated graphite

For an irreversibly exfoliated graphite, the tremendous sliding of the graphite layers has already occurred during the completed exfoliation, so no further tremendous sliding occurs upon subsequent mechanical stimulation (vibration). Nevertheless, the exfoliation process has irreversibly loosened the binding of the graphite layers to one another and, as a consequence, a small degree of sliding between the layers can easily occur upon subsequent mechanical vibration. This looseness is consistent with a very low elastic modulus in the direction perpendicular to the wall, as shown by instrumented nanoindentation testing [18]. The deformation upon nanoindentation is mostly reversible upon unloading, though the deformation magnitude during nanoindentation [18] is very large compared to that in dynamic mechanical testing [1]. Furthermore, no breakthrough of the graphite layers was observed during nanoindentation of exfoliated graphite [18], in contrast to the breakthrough observed in highly-oriented pyrolytic graphite by similar nanoindentation [19]. This suggests the essential reversibility of the small-amplitude dynamic sliding between the graphite layers during vibration. Even though the amplitude of the sliding is small, the sliding is easy and the back-and-forth sliding during vibration provides a significant degree of viscous behavior. It is akin to the wall of a balloon stretching and recoiling at a small deformation amplitude during repeated variation in the gas pressure in the balloon. Thus, the cell wall of exfoliated graphite provides a balloon-like interface-derived viscous behavior.

The degree of viscous behavior of the cell wall of irreversibly exfoliated graphite has been measured to be huge [1], in fact extraordinarily high among solid materials, including bulk rubber. The degree of viscous character is described by the loss tangent (i.e., $\tan \delta$, where δ is the phase lag between the stress wave and the strain wave during dynamic loading), which is equal to the ratio of the loss modulus to the storage modulus. An exfoliated graphite compact is formed by compressing pieces of exfoliated graphite, with each piece known as a worm, in the absence of a binder, such that the worms become connected during the compression through mechanical interlocking, which is enabled by the cellular structure of each worm. The solid part of an exfoliated graphite consists of cell walls. During dynamic flexure of an exfoliated graphite compact, the loss tangent of the cell wall (as given approximately by the loss tangent of the compact divided by the solid volume fraction) has been determined experimentally to be up to 35 (Fig. 5) [1], compared to a value of 0.7 for bulk rubber

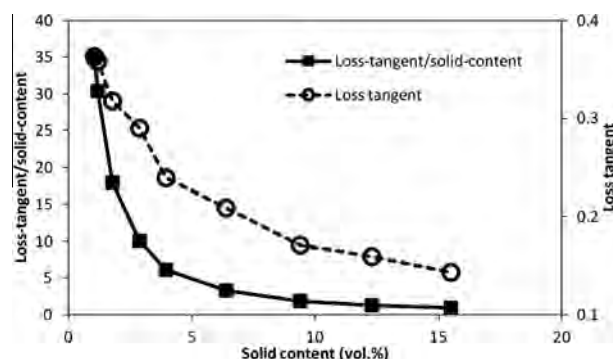


Fig. 5 – Dynamic flexural properties of exfoliated graphite compacts at various solid contents (solid volume fractions), with the static strain at 2%. The loss tangent and the loss tangent divided by the solid content are plotted. The loss tangent divided by the solid content relates to the degree of viscous character of the cell wall; its highest value of 35 occurs at the lowest solid content of 1 vol.% [1].

[20]. Upon dynamic compression (rather than flexure) of the exfoliated graphite compact, the loss tangent of the cell wall is up to 25 [1], which is less than the value of 35 obtained under flexure because the compact exhibits preferred orientation of the graphite layers in the plane perpendicular to the compaction direction and, compared to compression, flexure gives more shear stress in the plane of the graphite layers; the shear stress facilitates the sliding. Both values of 35 and 25 are extraordinarily high values among solid materials. The values decrease with increasing degree of compaction of the exfoliated graphite (i.e., with decreasing solid content in the compact) (Fig. 5), due to the associated decreasing ease of sliding between the layers as the compact becomes more tightly packed. This means that an adequate degree of looseness of the binding between the layers is required for the viscous behavior to be substantial. The extraordinarily high degree of viscous character is made possible by the balloon-like interface-derived viscous mechanism under the condition that the layers are sufficiently loosely bound. This interfacial mechanism results in energy loss due to the friction between the layers as sliding occurs. The greater is the friction, the higher is the mechanical energy loss (dissipation) for the same sliding amplitude. Indeed, a simple calculation has shown that the mechanical energy loss associated with the viscous character in a cell wall stems substantially from the friction [21].

Viscoelastic behavior includes viscous and elastic characters. In contrast to the viscous character, the elastic character of the cell wall, as shown by the storage modulus divided by the solid content [1], is essentially independent of the degree of compaction, weakening slightly with increasing degree of compaction. This means that the stiffness of the cell wall tends to decrease slightly with increasing solid content, presumably due to the defects generated in the graphite layers during compaction and the increase in the amount of defects as the compaction pressure increases. The loss modulus of the compact increases with increasing solid content [1]; this trend corroborates with the increase of the storage modulus of the compact with increasing solid content. However, the

loss-modulus/solid-content decreases with increasing solid content [1]; this trend corroborates with the decrease of the loss-tangent/solid-content with increasing solid content (Fig. 5). In other words, the loss modulus of the cell wall is mainly governed by the degree of viscous character, whereas the loss modulus of the compact is mainly governed by the stiffness of the compact.

Without exfoliation, the sliding is relatively difficult, due to the fact that the binding between the layers is too tight. Hence, the abovementioned viscous mechanism does not occur. Indeed, the degree of viscous character is small for graphite flakes that have not been exfoliated, as shown by similar dynamic mechanical testing.

Upon compression in the absence of a binder (i.e., without cement), exfoliated graphite forms a flexible sheet that is known as “flexible graphite” [22–28]. The sheet formation is due to the mechanical interlocking between the adjacent worms. The sheet exhibits preferred orientation of the graphite layers in the plane of the sheet, as indicated by the much lower in-plane electrical resistivity compared to the out-of-plane resistivity [27]. This preferred orientation and the cellular structure result in resiliency in the direction of the compression during sheet formation. The resiliency has enabled the application of flexible graphite as fluid gaskets [23] and EMI gaskets [26–28]. This resiliency, which is in the direction that is mainly perpendicular to the cell walls, is consistent with (i) the balloon-like interface-derived viscous behavior observed during dynamic loading [1], (ii) the essential reversibility of the nanoindentation deformation [18] and (iii) the reversibility of the conformability of the surface topography upon compression in the direction perpendicular to the sheet [29]. Flexible graphite that is available commercially differs from the exfoliated graphite compact (Fig. 5) [1] in that the degree of compaction is much greater. As a consequence of the decrease of the viscous character with increasing degree of compaction (Fig. 5), the loss tangent of flexible graphite that is available commercially is relatively low [30].

The balloon-like interface-derived viscous behavior discovered in exfoliated graphite is scientifically intriguing and technologically useful. This mechanism is in sharp contrast to the well-known bulk viscous behavior that rubber exhibits. The interface-derived viscous mechanism requires a large interface area, such that the interfaces are loose enough to allow easy sliding. The large-area interfaces can be provided by the interfaces in a nanoscale multilayer, which makes up the cell wall of exfoliated graphite. An advantage of the interfacial mechanism is that the interfaces do not necessarily decrease the stiffness of the material, since the constituent that provides the interfaces may serve as a reinforcement while the interfaces provide the viscous character. In contrast, the bulk viscous mechanism, as commonly achieved by including a rubber-like constituent in a material, causes the stiffness of the material to decrease. Stiffness is important for structural materials.

The parameters that affect the balloon-like interface-derived viscous behavior include (i) the cell wall length (which relates to the intercalate island length, which depends on the intercalate concentration in the reaction vessel during intercalation and on the stage of the intercalation compound,

and also relates to the graphite flake in-plane size), (ii) the ease of sliding between the graphite layers in the cell wall (the ease depending on the chemistry of the intercalated graphite, the extent of exfoliation and the tightness of the compaction of the exfoliated graphite), (iii) the average in-plane length of the graphite layers that make up a cell wall (this length presumably depending on the extent of in-plane defect formation during exfoliation), and (iv) the number of graphite layers in the cell wall (this number depending on the amount of expansion during exfoliation, such that the expansion amount depends on the intercalate species and the heating rate during exfoliation). The effects of these parameters still remain to be investigated for the purpose of unraveling the science of this extraordinary interface-derived viscous behavior.

4. Application to cement-matrix composites

With the incorporation of exfoliated graphite (8 vol.%) in a cement matrix, such that cell walls are sandwiched by the cement matrix, cement-based materials that exhibit loss tangent under flexure as high as 0.8 (Table 1) have been obtained [2]. Since the area of the interface between graphite and cement is small compared to that between the numerous (about 60) graphite layers in a cell wall, the viscous behavior is mainly due to the sliding between the layers in a cell wall. The degree of viscous character in the cement-based material is even greater than that of bulk rubber, the loss tangent of which is 0.7 (Table 1).

Constrained-layer damping involves the sandwiching of a viscous layer by stiff layers. A polymeric material is typically used as the viscous constrained layer [31–33]. Due to the significant variation of the viscous behavior of a polymer with temperature, the damping behavior varies considerably with the temperature and the temperature range for effective damping tends to be narrow [31,33]. In addition, the viscous layer tends to cause substantial reduction in the stiffness [33].

The incorporation of exfoliated graphite in cement amounts to constrained-layer damping in the microscale, with the constrained layer involving the interface-derived viscous mechanism rather than the conventional bulk viscous mechanism. Conventional constrained-layer damping involves components that are much larger in scale than the microscale. In contrast, in the exfoliated graphite cement-matrix composite, the microscale constrained-layer damping involves a large number of microscopic constrained layers that are distributed in a stiff (cement) matrix, which serves as the constituent that sandwiches each of the microscopic constrained layers.

Stiffness is required for a structural material. One disadvantage of the abovementioned cement-based material is that the stiffness is low compared to conventional cement-based materials. This issue has been resolved by the combined use of silica fume and exfoliated graphite [34]. Silica fume is fine noncrystalline silica produced by electric arc furnaces as a by-product of the production of metallic silicon or ferrosilicon alloys. It is a powder with particle size 100 times smaller than that of anhydrous Portland cement particles, i.e.,

Table 1 – Dynamic flexural properties obtained under three-point bending at 0.2 Hz and room temperature. All data were obtained using the same testing method in the author's laboratory. The bottom row gives the data for bulk rubber (without cement) [20], which is high in the loss tangent but low in the storage and loss moduli. All the other rows give data for cement-based materials [39] in the absence of aggregate. Plain cement paste (the second last entry) is low in the loss tangent, storage modulus and loss modulus. The top entry gives the data for exfoliated graphite (8 vol.%) cement-matrix composite [2], which is the highest in the loss tangent, storage modulus and loss modulus among all the entries.

Mechanism	Admixture	Loss tangent	Storage modulus (GPa)	Loss modulus (GPa)
Balloon-like interface-derived	Exfoliated graphite [2]	0.81	9.3	7.5
Interfacial friction	Silica fume [39]	0.11	5.8	0.62
	Carbon fiber [39]	0.11	3.2	0.35
Bulk viscous	Latex [39]	0.12	2.8	0.34
	Methylcellulose [39]	0.07	4.1	0.30
	Polyethylene fiber [39]	0.06	2.8	0.15
Interfacial friction + bulk viscous	Silica fume + methylcellulose [39]	0.11	6.2	0.65
Plain cement paste [39]		0.035	1.9	0.067
Bulk rubber [20]		0.67	0.0075	0.005

mean particle size between 0.1 μm and 0.2 μm . The SiO_2 content ranges from 85% to 98%. Due to its small particle size, silica fume is effective for refining the microstructure of a cement-based material, thereby enhancing the stiffness and strength [35–38]. In addition, the small particle size results in a substantial area of the interface between silica and cement and this enables a substantial degree of particulate interface-derived viscous character (Table 1) [39], which is to be distinguished from the balloon-like interface-derived viscous behavior. This means that the silica fume helps both the stiffness and the viscous character. Furthermore, silica fume addition causes reduction of the water permeability, thereby decreasing the tendency of embedded steel to be corroded [38]. Silica fume is pozzolanic [35], due to the cementitious character resulting from its surface reactivity, which relates to its amorphous structure.

A drawback is that silica fume addition degrades the workability of the cement mix, but this can be alleviated by the use of a water-reducing agent and/or silane surface treatment of the silica fume [39,40]. In addition, the silane treatment of silica fume enhances the viscous character of the resulting cement-matrix composite [34,40–43].

Due to the fact that the silica-cement interface area is much smaller than that of the cell wall of exfoliated graphite, the ability of silica fume to enhance the viscous character is considerably less than that of the cell wall of exfoliated graphite. The cell wall of exfoliated graphite is also expected to be more effective than carbon fibers, nanofibers and nanotubes, due to its larger interface area resulting from its multi-layer planar geometry. The exfoliation of intercalated carbon fibers (even those of the graphitic form) is much more difficult than that of intercalated graphite flakes and the degree of expansion is much lower [44]. Sliding at an interface between planar layers is expected to be easier than sliding at an interface between concentric cylinders in a nanotube. In contrast to the abovementioned interfacial mechanisms, latex (Table 1) [39] enhances the viscous character due to a bulk viscous mechanism associated with each latex particle. Compared to silica fume, latex is expensive.

In order for the cell wall of exfoliated graphite to be sufficiently tightly sandwiched by the cement matrix, as needed

for constrained-layer damping, the fabrication of the cement-based material requires compaction prior to curing. A process involves dry compaction of a mixture of cement particles and exfoliated graphite prior to exposure to water for curing the cement [2]. Simple addition of the exfoliated graphite to a cement mix does not provide the necessary squeezing, thus resulting in loose sandwiching of the exfoliated graphite by the cement matrix after curing and the near absence of constrained-layer damping [3]. Furthermore, without the squeezing, the exfoliated graphite units (worms) in the cement remain macroscopic and highly porous, making them ineffective for enhancing the strength. In contrast, with the squeezing, the exfoliated graphite is effective for enhancing the strength. Thus, the method of incorporating exfoliated graphite in cement is critical. In practice, the squeezing may be achieved by using roller compaction.

The mechanical interlocking ability of the worms enables them to be interconnected upon compression of a dry mixture of worms and cement particles, thereby resulting in a graphite network. The networking is supported by the low resistivity (0.04 $\Omega\text{ cm}$ perpendicular to the compression direction and 0.5 $\Omega\text{ cm}$ in the compression direction) [2]. In contrast, the resistivity is 480 $\Omega\text{ cm}$ for cement containing 37 vol.% graphite powder [45]. Although the networking itself is not expected to affect the viscous behavior, it affects the distribution of the exfoliated graphite in the cement-based material and may enable a coordinated viscous response among the cell walls of distinct worms in the cement-matrix composite. The possible effect of the networking on the viscous response remains to be investigated.

5. Further discussion

The dynamic mechanical properties reported in this paper were measured under dynamic loading using a sinusoidal stress wave at a controlled low frequency. This is the forced resonance method. The resulting sinusoidal strain wave is out of phase from the stress wave by a phase angle δ . A low frequency (e.g., 0.2 Hz) is used in order to allow accurate measurement of δ . The frequency is far from any resonance vibration frequency. That the loss tangent results obtained in this

way agrees with those obtained on larger specimens using the free resonance method (which involves the use of an impulse hammer) has been shown [46].

This paper addresses the elastic regime, due to its relevance to normal structural operation. Due to the nanoscale interfacial mechanism of damping, plastic deformation and damage may not affect the damping performance significantly. Damping in the plastic deformation and damage regimes is relevant to the mitigation of the hazard of extreme events (e.g., earthquake), but the science in the elastic regime is more fundamental.

Graphene in the form of single atomic graphite layers, if well dispersed in a matrix, can provide much interface area between it and the matrix. Slight sliding at this interface potentially provides a degree of viscous behavior, which is distinct in mechanism from the balloon-like interface-derived viscous behavior.

A graphite nanoplatelet [47–49] is in the form of a stack of graphite layers and is commonly made by the breaking up of exfoliated graphite by mechanical agitation (e.g., sonication). If the nanoplatelets are dispersed in a matrix, they can provide viscous behavior due to the area associated with the interface between the graphite layers in each nanoplatelet, in addition to the interface between each nanoplatelet and the matrix. However, with the cell walls greatly broken down in the in-plane direction during the preparation of graphite nanoplatelets [47,49], the length-to-thickness aspect ratio of the graphite layer stack is expected to be much reduced. This aspect ratio reduction is expected to increase the need for a strong bond between the graphite and the matrix in order for the load transfer to be effective enough for constrained-layer damping. In other words, for the same bond strength, the viscous behavior is expected to decrease when the aspect ratio is reduced. Furthermore, since the mechanical agitation used to prepare the nanoplatelets has already caused fracture at the relatively loose interfaces, the layers in a nanoplatelet may not be sufficiently loose from one another.

6. Conclusion

It has been recently reported that exfoliated graphite exhibits an extraordinarily strong viscous behavior, such that the loss tangent of the cell wall in the cellular structure of exfoliated graphite is as high as 35 under flexure [1]. The exfoliated graphite is obtained by the rapid heating of acid-intercalated graphite flakes. It exhibits a cellular microstructure, with about 60 graphite layers in the cell wall. It has also been reported that suitable incorporation of exfoliated graphite in a cement-matrix composite results in a material that exhibits high values of both the loss tangent and the storage modulus, and hence an extraordinarily strong vibration damping behavior [2].

This paper has provided explanation of the abovementioned extraordinary viscoelastic behaviors. The strong viscous behavior of exfoliated graphite is explained in terms of a balloon-like interface-derived viscous deformation mechanism. This mechanism is associated with the dynamic sliding at low amplitudes between the graphite layers in the cell wall of exfoliated graphite during dynamic loading in

the elastic regime. The ease of sliding is enabled by the loosening of the interlayer interface that has occurred during exfoliation, in which the cell wall extends greatly like a balloon due to extensive sliding between the graphite layers in the cell wall. Without the loosening, the viscous behavior is weak. Consistent with the requirement of looseness is that the degree of viscous character of exfoliated graphite decreases with increasing degree of compaction of the exfoliated graphite.

Flexible graphite is a sheet made by greatly compressing exfoliated graphite without a binder. The viscous behavior of exfoliated graphite is consistent with the well-known resiliency of flexible graphite in the direction perpendicular to the plane of the sheet.

In the cement-matrix composite, the exfoliated graphite is sandwiched with sufficient tightness by the cement matrix in the microstructure of the composite, thereby providing constrained-layer damping in the microscale. In conventional constrained-layer damping, the constrained layer, typically polymeric, is macroscopic and viscous, such that the viscous behavior is due to the bulk viscous deformation mechanism. In contrast, in the cement-matrix composite, the constrained layer is microscopic and distributed, and exhibits balloon-like interface-derived viscous behavior. Without sufficient tightness in the sandwiching of the exfoliated graphite by the cement matrix, the exfoliated graphite remains highly porous and both constrained-layer damping and strengthening are ineffective. The tight sandwiching can be achieved by the compression of a dry mixture of exfoliated graphite and cement particles prior to curing the cement in the presence of water.

REFERENCES

- [1] Chen P, Chung DDL. Viscoelastic behavior of the cell wall of exfoliated graphite. *Carbon* 2013;61:305–12.
- [2] Muthusamy S, Wang S, Chung DDL. Unprecedented vibration damping with high values of loss modulus and loss tangent, exhibited by cement-matrix graphite network composite. *Carbon* 2010;48(5):1457–64.
- [3] Chen P, Chung DDL. Comparative evaluation of cement-matrix composites with distributed versus networked exfoliated graphite. *Carbon* 2013;63:446–53.
- [4] Chung DDL. Graphite. *J Mater Sci* 2002;37(8):1475–89.
- [5] Inagaki M, Kang F, Toyoda M. Exfoliation of graphite via intercalation compounds. *Chem Phys Carbon* 2004;29:1–69.
- [6] Chung DDL. Exfoliation of graphite. *J Mater Sci* 1987;22(12):4190–8.
- [7] Celzard A, Mareche JF, Furdin G. Modelling of exfoliated graphite. *Prog Mater Sci* 2005;50(1):93–179.
- [8] Dresselhaus MS, Dresselhaus G. Intercalation compounds of graphite. *Adv Phys* 2002;51(1):1–186.
- [9] Guerard D, Fuzellier H. The graphite intercalation compounds and their applications. *Condens Syst Low Dimens* 1991;253:695–707.
- [10] Herold A, Petitjean D, Furdin G, Klatt M. Exfoliation of graphite intercalation compounds: classification and discussion of the processes from new experimental data relative to graphite-acid compounds. *Mater Sci Forum* 1994;152–153(Soft Chemistry Routes to New Materials):281–7.

- [11] Saidaminov MI, Maksimova NV, Sorokina NE, Avdeev VV. Effect of graphite nitrate exfoliation conditions on the released gas composition and properties of exfoliated graphite. *Inorg Mater* 2013;49(9):883–8.
- [12] Daumas N, Herold A. Relations between phase concept and reaction mechanics in graphite insertion compounds. *C R Hebd Sean Acad Sci, Serie C* 1969;268:373–82.
- [13] Heerschap M, Delavignette P, Amelinckx S. Electron microscope study of interlamellar compounds of graphite with bromine, iodine monochloride and ferric chloride. *Carbon* 1964;1:235–8.
- [14] Heerschap M, Delavignette P. Electron-microscopy study of the ferric chloride/graphite compound. *Carbon* 1967;5:383–4.
- [15] Anderson SH, Chung DDL. Exfoliation of intercalated graphite. *Carbon* 1984;22(3):253–63.
- [16] Anderson SH, Chung DDL. Exfoliation of single crystal graphite and graphite fibers intercalated with halogens. *Synth Met* 1983;8:343–9.
- [17] Chung DDL. Intercalate vaporization during the exfoliation of graphite intercalated with bromine. *Carbon* 1987;25(3):361–5.
- [18] Chen P, Chung DDL. Elastomeric deformation of exfoliated graphite. *Carbon*, submitted for publication
- [19] Richter A, Ries R, Smith R, Henkel M, Wolf B. Nanoindentation of diamond, graphite and fullerene films. *Diam Relat Mater* 2000;9(2):170–84.
- [20] Fu W, Chung DDL. Vibration reduction ability of polymers, particularly polymethylmethacrylate and polytetrafluoroethylene. *Polym Polym Compos* 2001;9(6):423–6.
- [21] Chen P, Chung DDL, private communication.
- [22] Ionov SG, Avdeev VV, Kuvshinnikov SV, Pavlova EP. Physical and chemical properties of flexible graphite foils. *Mol Cryst Liq Cryst Sci Technol* 2000;A 340:349–54.
- [23] Chung DDL. Flexible graphite for gasketing, adsorption, electromagnetic interference shielding, vibration damping, electrochemical applications, and stress sensing. *J Mater Eng Perform* 2000;9(2):161–3.
- [24] Chugh R, Chung DDL. Flexible graphite as a heating element. *Carbon* 2002;40(13):2285–9.
- [25] Chen P, Chung DDL. Dynamic mechanical properties of flexible graphite made from exfoliated graphite. *Carbon* 2012;50:283–9.
- [26] Luo X, Chugh R, Biller BC, Hoi YM, Chung DDL. Electronic applications of flexible graphite. *J Electron Mater* 2002;31(5):535–44.
- [27] Luo X, Chung DDL. Electromagnetic interference shielding reaching 130 dB using flexible graphite. *Carbon* 1996;34(10):1293–4.
- [28] Chung DDL. Electromagnetic interference shielding effectiveness of carbon materials. *Carbon* 2001;39(2):279–85.
- [29] Luo X, Chung DDL. Flexible graphite under repeated compression studied by electrical resistance measurements. *Carbon* 2001;39(7):985–90.
- [30] Luo X, Chung DDL. Vibration damping using flexible graphite. *Carbon* 2000;38(10):1510–2.
- [31] Das R, Kumar R, Kundu PP. Vibration damping characterization of linseed oil-based elastomers for its effectiveness to attenuate structural vibration. *J Appl Polym Sci* 2013;130(5):3611–23.
- [32] Lu P, Liu XD, Ma X, Huang WB. Analysis of damping characteristics for sandwich beams with a polyurea viscoelastic layer. *Adv Mater Res* 2012;374–377(Pt. 2, Sustainable Development of Urban Environment and Building Material):764–9.
- [33] Segiet M, Chung DDL. Discontinuous surface-treated submicron-diameter carbon filaments as an interlaminar filler in carbon fiber polymer-matrix composites for vibration reduction. *Compos Interfaces* 2000;7(4):257–76.
- [34] Chen P, Chung DDL. Mechanical energy dissipation using cement-based materials with admixtures. *ACI Mater J* 2013;110(3):279–90.
- [35] Pourkhorshidi AR, Najimi M, Parhizkar T, Hillemeier B, Herr R. A comparative study of the evaluation methods for pozzolans. *Adv Cement Res* 2010;22(3):157–64.
- [36] Saje D, Saje F, Lopatic J. Compressive strength of concrete containing silica fume. *J Mech Behav Mater* 2009;19(6):355–64.
- [37] Daou F, Piot B. Cement-slurry performance and set-cement properties vs microsilica densification. *SPE Drill Completion* 2009;24(4):590–8.
- [38] Chung DDL. Improving cement-based materials by using silica fume. *J Mater Sci* 2002;37(4):673–82.
- [39] Fu X, Chung DDL. Vibration damping admixtures for cement. *Cem Concr Res* 1996;26(1):69–75.
- [40] Xu Y, Chung DDL. Improving silica fume cement by using silane. *Cem Concr Res* 2000;30(8):1305–11.
- [41] Xu Y, Chung DDL. Cement-based materials improved by surface treated admixtures. *ACI Mater J* 2000;97(3):333–42.
- [42] Liu T, Ou J. Effects of silane-treated silica fume on damping property of cement mortar. *Proceedings RILEM, PRO 32 (International Conference on Advances in Concrete and Structures, Vol. 1), 2003: 168–176.*
- [43] Ou J, Liu T, Li J. Analysis of the damping behavior and microstructure of cement matrix with silane-treated silica fume. *J Wuhan Univ Technol, Mater Sci Ed* 2006;21(2):1–5.
- [44] Anderson SH, Chung DDL. Graphite ribbons formed from graphite fibers. *Carbon* 1984;22(6):613–4.
- [45] Wen S, Chung DDL. Thermoelectric behavior of carbon-cement composites. *Carbon* 2002;40(13):2495–7.
- [46] Zou D, Liu T, Teng J, Leng J, Asundi AK, Wolfgang E. Improving the damping ability by the addition of Nano SiO₂ to the concrete materials. *Proceedings of SPIE, 7493, Pt. 2, Second International Conference on Smart Materials and Nanotechnology in, Engineering, 2009:74933C/1-74933C/9.*
- [47] Lin C, Chung DDL. Graphite nanoplatelet pastes versus carbon black pastes as thermal interface materials. *Carbon* 2009;47(1):295–305.
- [48] Li B, Zhong W. Review on polymer/graphite nanoplatelet nanocomposites. *J Mater Sci* 2011;46(17):5595–614.
- [49] Xiang J, Drzal LT. Thermal conductivity of exfoliated graphite nanoplatelet paper. *Carbon* 2011;49(3):773–8.